Inverse Estimation of Time-Dependent Heat Flux in Stagnation Region of Annular Jet on a Cylinder Using Levenberg–Marquardt Method

Montazeri, Mostafa;Mohammadiun, Hamid*[+]; Mohammadiun, Mohammad; DibaeeBonab; Mohammad Hossein

Department of Mechanical Engineering, Shahrood Branch, Islamic Azad University, Shahrood, I.R. IRAN

Vahedi, Mojtaba

Department of Electrical Engineering, Shahrood Branch, Islamic Azad University, Shahrood, I.R. IRAN

ABSTRACT: *All solving methods available in the literature are formulated for direct solution of stagnation point flow and its heat transfer impinging on the surfaces with known boundary conditions. In this study for the first time, an anumerical code based on Levenberg–Marquardt method is presented for solving the inverse heat transfer problem of an annular jet on a cylinder and estimating the time-dependent heat flux using temperature distribution at a specific point. Also, the effect of noisy data on the final results is studied. For this purpose, the numerical solution of the dimensionless temperature and the convective heat transfer in a radial incompressible flow on a cylinder rod is carried out as a direct problem. In the direct problem, the free stream is steady with an initial flow strain rate of□. Using similarity variables and appropriate transformations, momentum and energy equations are converted into Semi-similar equations. The new equation systems are then discretized using an implicit finite difference method and solved by applying the Tri-Diagonal Matrix Algorithm (TDMA). The heat flux is then estimated by applying the Levenberg–Marquardt parameter estimation approach. This technique is an iterative approach based on minimizing the least-square summation of the error values, the error being the difference between the estimated and measured temperatures. Results of the inverse analysis indicate that the Levenberg–Marquardt algorithm is an efficient and acceptably stable technique for estimating heat flux in axisymmetric stagnation flow. This method also exhibits considerable stability for noisy input data. The maximum value of the sensitivity coefficient is related to the estimation of exponential heat flux and its value is 0.1619 also the minimum value of the sensitivity coefficient is 5.62×10^{-6} which is related to the triangular heat flux. The results show that the parameter estimation error in calculating the triangular and trapezoidal heat flux is greater than the exponential and sinus–cosines heat flux because the maximum value of RMS error is obtained for these two cases, which are 0.481 and 0.489, respectively the reason for the increase in the errors in estimating these functions is the existence of points where the first derivative of the function does not exist. The problem is particularly important in pressure-lubricated bearings.*

KEYWORDS: *Inverse heat transfer; Levenberg–Marquardt method; Time-dependent heat flux; Annularjet; Semi-similar solution; Noisy data.*

To whom correspondence should be addressed.
+E-mail: hmohammadiun@iau-shahrood.ac.ir
1021-9986/2022/3/971-988 18/$/6.08

INTRODUCTION

While it is relatively simple to measure temperature (e.g., with thermocouples, infrared cameras, or Resistance Temperature Detectors (RTDs)), it is challenging to measure heat fluxes, especially in operating devices. Direct heat transfer problem involves determining the temperature of internal points of a region when the initial and boundary conditions, as well as the thermo-physical characteristics, heat generation, heat flux, or the wall temperature, are known [1]. Unlike direct problems, inverse heat transfer problems are defined as the estimation of initial and boundary conditions, material characteristics, source and sink terms, and governing equations by considering the distribution of the measured temperature in one or more internal points [2].

Because of the solution stability, inverse problems are much harder to solve compared to direct problems. Mathematically, these types of problems are called ill-posed problems. In recent decades, through the emerging advanced computers, inverse solution techniques have gained a more general application beyond heat transfer problems. For example, some of the main applications of inverse heat transfers include cooling control of electrical equipment, estimation of cooling jet velocity in machining and quench hardening process, determination of boundary conditions between mold and the molten metal in casting velocity in machining and quench hardening process, determination of boundary conditions between mold and the molten metal in casting and rolling processes [3], heat flux determination on a wall surface exposed to fire or inside the surface of a combustion chamber [4] as well as the surfaces where ablation or melting occurs [5]. Other uses of inverse heat transfer include prediction of the internal wall of reactors, determining thermal conduction coefficient and the external surface conditions in the re-entry of a space vehicle, temperature or heat flux distribution modeling at the tool-work interface of machine cutting [6], and cooling control problems [7]. Different solution methods are applied to inverse heat transfer problems, some of which include exact solutions, inverse transform of Duhamel integral, Laplace transformation, control volume method, Helmholtz equations, finite difference, finite element approximation, digital filter synthesis, Tikhonov regularization, Elifanov iteration method, conjugate gradient, and Levenberg–Marquardt methods [8]. Levenberg–Marquardt method is an iterative inverse algorithm based on minimizing the least-square summation of the error values and is employed in this paper.

Jiang et al. [9] obtained the time-dependent boundary heat flux on a solid bar using the conjugate gradient method with an adjoint equation and zeroth-order Tikhonov regularization approach to make the inverse solution stable. In their work, a finite difference method was used to solve the problem.

Chen et al. [10] derived the temperature and heat flux distribution of the quenching surface using the inverse technique. They utilized the conjugate gradient method for improved temperature and heat flux estimation for a two-dimensional problem on cylindrical coordinates. Finite element techniques were employed to solve the governing equations.

Plotkowski and *Krane* [11] examined the use of inverse heat conduction models to estimate the transient heat flux in electro slag remelting. They studied three inverse heat transfer methods for industrial applications.

Hsu et al. [12]applied the inverse problem on wall heat flux estimation to film-wise condensation on a vertical surface. Their inverse method does not require prior knowledge of the functional form of unknown variables.

Khaniki and *Karimian* [13] used temperature data to get the heat flux absorbed on a satellite surface. They proposed a simple heat flux sensor to examine the related probable limitations. Using the temperature data, they also proposed an inverse solution to the energy equation which yields the heat flux absorbed on the satellite surface.

Beck et al. [14] conducted some research into the estimation of heat flux entering the surface of a body using the inverse approach. Their calculation method used the measured temperature data of the internal points.

Liu [15]developed a hybrid mechanism to simultaneously identify the thermal conductivity and heat capacity in an inverse heat flux problem. This mechanism was a combination of the genetic and Levenberg–Marquardt algorithms. *Mohammadiun et al.* [16] estimated the time-dependent heat flux using temperature at a specific point. Their method included the use of the finite difference method to solve the governing equations.

Tai et al. [17] applied an inverse conduction heat transfer method to estimate the spatial and temporal variation of heat flux on the drilled-hole wall surfaces. Their approach utilized the internal temperature of the body

measured by thermocouples and the governing equations were solved by the finite element method.

Rahimi et al. [18] estimated the time-dependent strength of a heat source using temperature distribution at a point in a three-layer system.

Mohammadiun et al. [19] used the sequential function specification method for heat flux prediction on the sublimation boundaries of decomposing materials. They used the inverse method to predict thermal boundary conditions on the surface.

In another study, *Mohammadiun et al.* [20] applied a sequential function specification method to ablative surfaces. The inverse method has been used in the mentioned study to estimate heat flux at the moving interface.

Wu et al. [21] proposed an inverse algorithm based on the conjugate gradient method to solve the hyperbolic heat conduction problem and estimate the unknown heat flux on an infinite cylinder. The measured internal temperatures were used for this purpose.

Recently, new inverse heat transfer methods applied to microelectronics are combined with a non-linear approach to calculate the sensitivity coefficients concerning the heat flux. A correction for convective heat transfer, which only depends on the gas-to-wall temperature difference, has been presented by *Cuadrado et al.* [22]. Their methodology was validated using numerical and experimental tests, considering only conduction and also fully conjugate heat transfer analysis.

Duda [23] proposed a method for simplification of three-dimensional transient heat conduction by reduction to an axisymmetric problem with a new inverse method solution. In this research the 3-D problem has been simplified to an axisymmetric analysis and a method has been presented for solving the axisymmetric IHCP in a complex domain based on the control volume finite element method.

A technique of resolving the nonlinear three-dimensional IHCP with complex geometry to determine an unknown time-dependent surface heat flux of the system in the online mode is proposed by *Huang et al.* [24]. They developed an adaptive sequential Tikhonov regularization method to obtain the heat flux component sequentially and a fast and accurate method, based on an Artificial Neural Network (ANN), was used for the direct solution.

The developed algorithm for solving the inverse problems for models based on fractional derivatives has been presented by *Brociek et al.* [25]. They showed that this algorithm can reconstruct boundary conditions and some other model parameters (e.g. physical parameters of the material), and the number of restored parameters can be arbitrary.

Perakis et al. [26] applied an inverse method for estimating the spatially resolved heat flux distribution at the hot gas wall of multi-element, actively cooled engines using the information provided by temperature measurements in the material. In their study, the inverse heat transfer method implemented in Roq_FITT is intended for the analysis of temperature and heat flux distribution.

Numerical solution of hydrodynamics and heat transfer of the laminar incompressible flow around a single diamond-shaped cylinder at moderate Reynolds number ($1 \leq Re \leq 70$) and a Prandtl number of $Pr=0.7$ on a large range of apex angle ($33 \leq \alpha \leq 120°$) has been studied by *Sochinskii et al.* [27]. They used the finite volume method in 2D with OpenFoam to solve the conservation equations.

A solution to Navier-Stokes equations generally involves high mathematical complexity. This is due to the nonlinearity of these equations such that the superposition theory, used for potential flow, is not applicable. However, in some cases, the exact solution to Navier-Stokes can be obtained when the nonlinear advection terms are naturally eliminated. The exact solution to the stagnation flow problem was initially achieved by *Hiemenz* [28]. He examined two-dimensional stagnation flow against a flat plate and assumed the stagnation flow on the flat plate to be laminar, incompressible, and steady. Using a suitable variable and converting velocity components to a similarity function, Hiemenz reached an ordinary differential equation and derived the velocity field and pressure field in the vicinity of the flat plate.

Following Hiemenz, *Homann* [29] achieved an exact solution to the three-dimensional Navier-Stokes equations for axisymmetric stagnation flow against a flat plate. Using an appropriate change of variables and transforming velocity components into a similarity function, Homann reached an ordinary differential equation for the similarity function with a relevant power series solution. *Howarth* [30] and *Davey* [31] reported their research on the three-dimensional stagnation flow against a flat plate for nonaxisymmetric cases. The first exact solution to axisymmetric stagnation flow on an infinite cylinder was reported by *Wang* [32]. He assumed a stationary cylinder

with no rotational or axial movement and no suction and blowing on the cylinder wall. A radial axisymmetric flow perpendicular to the axis was assumed. Also, due to the symmetry of the free stream concerning the cylinder axis and considering a steady flow, all derivatives with respect to φ (angular direction) and t (time) are zero and the Navier-Stokes equations are simplified in cylindrical coordinates. In a series of studies [33-36], Gorla analyzed the axisymmetric stagnation flow around a cylinder with laminar flow in steady and transient states. In these works, the effect of uniform axial movement as well as the harmonic axial movement of the cylinder was studied. *Cunninget al.* [37] researched the effect of cylinder rotation with constant angular velocity on the stagnation flow over the cylinder. In this research, the effect of uniform suction and blowing on the cylinder wall was also considered. Due to cylinder rotation, the flow is entirely three-dimensional with the velocity also existing inφ direction. *Takhar et al.* [38] evaluated the effect of unsteady axisymmetric radial stagnation flow on the cylinder together with the effect of variable-speed axial cylinder movement. In their research, to reach a self-similar solution, the time-dependent functions related to the free stream and axial velocity of the cylinder are assumed in the form of inverse linear functions of time.

Saleh and *Rahimi* [39-41] reached exact solutions for axisymmetric stagnation flows on an infinite cylinder and the related heat transfer for cases where the cylinder has time-dependent axial and rotational movement. Further, *Shokrgozarabbasi* and *Rahimi* [42-45] proposed an exact solution to the three-dimensional stagnation flow and the transient heat transfer of viscous flow impinging on a flat plate. Also, in a series of studies [46-49], *Mohammadiun et al.* proposed self-similar solutions of radial stagnation point flow and heat transfer of a viscous, compressible fluid impinging on a cylinder in a steady state. They further studied the axisymmetric stagnation flow of a nanofluid on a cylinder for a steady flow when the cylinder wall is exposed to both constant heat flux and constant temperature [50,51]. *Zahmatkesh et al.* [52] evaluated the rate of entropy generation in an axisymmetric stagnation flow of Aluminum oxide nanofluid on a stationary cylinder. The effect of uniform suction and blowing as well as the volume fraction of the nanoparticles on the rate of entropy generation is also studied in the mentioned work.

Combined heat and mass transfer and thermodynamic irreversibilities in the stagnation point flow of Casson rheological fluid over a cylinder with catalytic reactions and inside a porous medium under local thermal non-equilibrium has been investigated by *Alizadeh et al.*[53].

Some valuable studies on direct solution problems can be found in the following references.

Heat and mass transfer effects in three-dimensional mixed convection flow of Eyring Powell over an exponentially stretching surface with convective boundary conditions have been investigated by *Bilal et al.* [54] In this research, the leading boundary layer partial differential equations have been reduced to the ordinary differential equations and numerically solved by using the Finite Element Method.

Recently *Nematollahzadeh et al.* have presented an exact analytical solution for the convective heat transfer equation from a semi-spherical fin. They compared exact solutions with numerical results such as the finite difference method and midpoint method with Richardson extrapolation[55].

A code based on the finite element method has been developed by *Madelatparvar et al.*[56] to predict the final scaffold structure made by the freeze-drying method. They studied the effect of material and processing parameters on the microstructure of the resulted scaffold.

A Computational Fluid Dynamics (CFD) analysis was performed for granular flow in an industrial screw feeder to study the choking phenomena by *Hussain et al.*[57]. Variation of mass flow through a change in Revolution per Minute (RPM) and moisture content was studied in this work.

A direct solution of the momentum and energy equations based on the similarity solution technique has been presented to solve the problem of the stagnation point flow of nanofluid on a cylinder with uniform transpiration by *Zahmatkesh et al.* [62]. A new inverse heat transfer method applied to microelectronics combines with a non-linear approach to calculate the sensitivity coefficients with respect to the heat flux and a correction for convective heat transfer, which only depends on the gas-to-wall temperature difference has been presented by *Cuadrado et al.* [63]. Their methodology was validated using numerical and experimental tests, considering only conduction and also fully conjugate heat transfer analysis.

Numerical simulation has been applied to investigate the pulsatile flow and heat transfer of a micropolar fluid

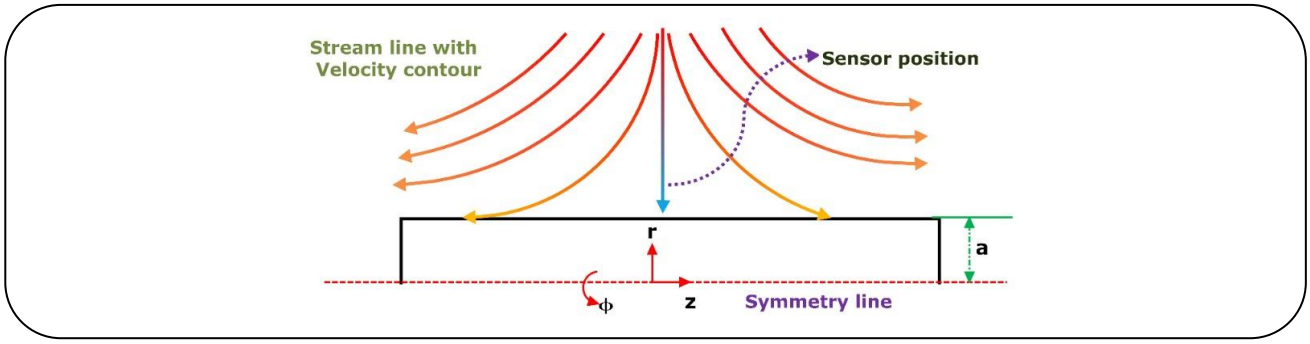

Fig. 1: The problem geometry and sensor position.

in a Darcy-Forchhmeir porous channel with transpiration at the wall by *Ashraf et al.* [64]. A mathematical model for the prediction of internal recirculation of complex impinging stream reactors has been presented by *Safaei et al.* [65].

Habibi et al. [66] investigated the viscosity uncertainty in the floating-axis fluid flow and heat transfer along a horizontal hot circle cylinder immersed in a cold Al_2O_3 water nanofluid.

As can be seen, inverse heat transfer in the vicinity of the stagnation region of an annular jet has not been considered in the literature yet. All articles on stagnation point flow only deal with the direct problem with known boundary conditions. However, in many real cases; accurate information about wall heat flux is not available therefore in this paper, for the first time, a numerical code based on Levenberg–Marquardt method is proposed to solve the inverse time-dependent boundary heat flux in the stagnation region of an annular jet on a cylinder. The algorithm uses the temperature distribution at appointing with a semi-similar solution. At every time step, the governing equations are converted to a system of coupled ordinary differential equations which, through discretization using the implicit finite difference method, are solved by the Tri-Diagonal Matrix Algorithm (TDMA). Sensitivity to noisy data is also evaluated. The results demonstrate considerable stability of the proposed method to noisy data.

PROBLEM FORMULATION

Direct solution

The geometry of the considered problem is depicted in Fig. 1. As shown, the flow is axisymmetric in cylindrical coordinates (r,z) with corresponding velocity components (u, w). Time-dependent heat flux is applied on the outer surface of the cylinder. We intend to determine the unknown heat flux $q_w(t)$ within$0 \le t \le t_f$ based on temperature distribution at a point. The input data may contain noise. The semi-similar solution method is employed in the numerical code to calculate temperature distribution. In this method, using dimensionless radius and transfer functions, partial differential equations are converted to ordinary differential equations which are then solved numerically.

The following items are some of the stagnation flow applications over a cylinder: the analysis of centrifugal machinery movement, heating, and cooling procedures, bearing lubrication, and cooling of drilling tools.

Governing equations

As shown in Fig. 1, the flow is considered in cylindrical coordinates (r, z) with corresponding velocity components (u, w). The flow is assumed incompressible and in a transient state. Considering axial symmetry, the governing equations in cylindrical coordinates will be as follows:

Continuity equation

$$\frac{\partial}{\partial r}(ru) + r\frac{\partial w}{\partial z} = 0 \tag{1}$$

Momentum equation in redirection

$$\frac{\partial u}{\partial t} + u\frac{\partial u}{\partial r} + w\frac{\partial u}{\partial z} = -\frac{1}{\rho}\frac{\partial P}{\partial r} + \upsilon\left(\frac{\partial^2 u}{\partial r^2} + \frac{1}{r}\frac{\partial u}{\partial r} - \frac{u}{r^2} + \frac{\partial^2 u}{\partial z^2}\right) \tag{2}$$

Momentum equation in the z-direction

$$\frac{\partial w}{\partial t} + u\frac{\partial w}{\partial r} + w\frac{\partial w}{\partial z} = -\frac{1}{\rho}\frac{\partial P}{\partial z} + \upsilon\left(\frac{\partial^2 w}{\partial r^2} + \frac{1}{r}\frac{\partial w}{\partial r} + \frac{\partial^2 w}{\partial z^2}\right) \tag{3}$$

In the above equations, ρ and $(\upsilon = \mu / \rho)$ are the fluid density and its kinematic viscosity, respectively.

Energy equation:

$$\frac{\partial T}{\partial t} + u\frac{\partial T}{\partial r} + w\frac{\partial T}{\partial z} = \bar{\alpha}\left(\frac{\partial^2 T}{\partial r^2} + \frac{1}{r}\frac{\partial T}{\partial r} + \frac{\partial^2 T}{\partial z^2}\right) \quad (4)$$

Where $\bar{\alpha} = \frac{k}{\rho C_p}$ is the fluid thermal diffusivity coefficient.

Boundary conditions for the momentum equations consist of the following:

$$r = a \;:\; u = 0 \;,\; w = 0 \quad (5)$$

$$r \to \infty \;:\; \frac{\partial u}{\partial r} = -\bar{k} \;,\; w = 2\bar{k}z \quad (6)$$

Equation (5) is the no-slip boundary condition of viscous fluid at the wall. Equation (6) is obtained from the inviscid solution of potential flow. The first term in (6) implies that the gradient of velocity *u* in distant regions is similar to that in potential flow. The second term in (6)reflects the fact that in points sufficiently far from the cylinder wall, the viscous fluid velocity *w* is the same as that for potential flow.

Boundary conditions to solve the energy equation are:

$$r = a : \quad \frac{\partial T}{\partial r} = -\frac{q_w(t)}{k} \quad (7)$$

$$r \to \infty : \quad T = T_\infty$$

In the above equations, *k* is the fluid's thermal conductivity and $q_w(t)$ is the time-dependent heat flux on the cylinder wall. Also, T_∞ is the constant temperature of the free stream.

The variables in the governing equations can be reduced. Using the inviscid solution patterns of (6) and multiplying by appropriate transfer functions, the below equations are proposed to reduce Navier-Stokes equations to dimensionless semi-similar equations:

$$u = -\bar{k}\frac{a}{\sqrt{\eta}} f(\eta,\tau) \;,\; w = 2\bar{k} f'(\eta,\tau) z \;,\; P = \rho \bar{k}^2 a^2 p \quad (8)$$

Where $\tau = 2k\Box t$ and $\eta = (r/a)^2$ are dimensionless time and dimensionless radius, respectively and ( )' denotes the derivative concerning variable η. Equations (8) automatically satisfy the continuity equation and by substituting them into momentum equations in *z* and *r* directions, for every time step,an ordinary differential equation is obtained, as below, to calculate *f*:

$$\eta f''' + f'' + Re\left[1 - (f')^2 + f f'' - \frac{\partial f'}{\partial \tau}\right] = 0 \quad (9)$$

Where $Re = k\Box a^2 / 2\upsilon$ is the Reynolds number. Using (5) and (6), the boundary conditions for (9) are obtained as:

$$\eta = 1 : \quad f = 0, \quad f' = 0 \quad (10)$$

$$\eta \to \infty : \quad f' = 1$$

To convert the energy equation, the dimensionless temperature $\theta(\eta, \tau)$ is used as:

$$\theta(\eta,\tau) = \frac{T(\eta,\tau) - T_\infty}{a\, q_w(\tau)/2k} \quad (11)$$

Using (8) and (11), the energy equation will be:

$$\eta\theta'' + \theta' + Re\,Pr\left(f\theta' - \frac{\partial\theta}{\partial\tau} - \frac{dq_w(\tau)/d\tau}{q_w(\tau)}\theta\right) = 0 \quad (12)$$

Boundary and initial conditions for (12) are:

$$\theta'(1,\tau) = -1 \;,\; \theta(\infty,\tau) = 0 \quad (13)$$

$$\theta(\eta,0) = \theta_{steady-state}$$

As shown in Fig. 1, the axisymmetric flow is injected into the cylinder in all directions. The Prandtl number is Pr=0.7 and the free stream temperature is $T_\infty = 30\,^\circ c$ with the sensor positioned as shown in the figure.

Validation of direct solution

An analytical solution for the steady-state problem of annular axisymmetric stagnation flow toward the moving cylinder for low and high Reynolds numbers has been extracted by *Wang et al.* [61]. The results of their analytical solution have been applied to the validation of the numerical procedure employed in this paper. As can be seen in Fig.2, the radiuses of inner and outer cylinders are *R* and *bR*, respectively and the inner cylinder (shaft) has been enclosed by the outer cylinder (bushing).

Asymptotic solution for small Reynolds numbers

When *W*=0 and Ω=0, the following expansion in terms of small Reynolds number (Re<<1) has been applied

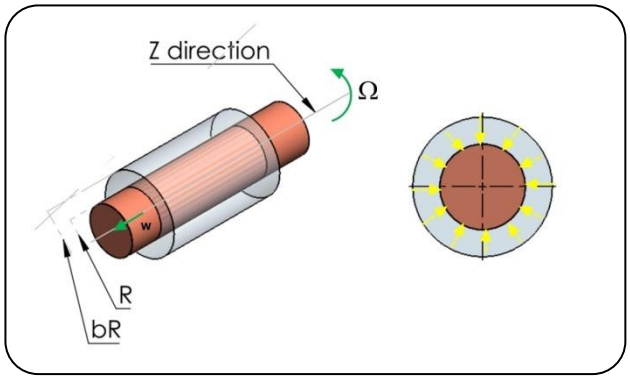

Fig. 2: Three-dimensional view of annular axisymmetric stagnation flow.

To calculate dimensionless function *f* in terms of the radial velocity component.

$$f = f_0 + Re f_1 + \dots \tag{14}$$

Analytical solution of zeroth-order and first-order equations [61] leads to the following relations for f_1 and f_0:

$$f_0 = \frac{\sqrt{b}[-2(b-1)\eta \ln \eta + \ln b.\eta^2 + 2(b-1-\ln b)\eta - (2b-2-\ln b)]}{(b-1)[2(b-1)-(b+1)\ln b]} \tag{15}$$

$$f_1 = C_2 + C_3\eta + C_4\eta^2 + \tag{16}$$

$$[288(-1+b)^2 b\eta^2 + 72C_1(-1+b)^4\eta -$$
$$108(-1+b)b\ln b.\eta^2 + 5(-1-b)b\ln b.\eta^3 -$$
$$72C_1(-1+b)^3(1+b)\ln b.\eta -$$
$$6b\ln^2 b.\eta^3 + b\ln^2 b.\eta^4 + 18C_1(-1+b^2)\ln^2 b.\eta -$$
$$72(-1+b)^2\eta(3b\eta + C_1 - 2bC_1 + b^2C_1)\ln\eta -$$
$$6(-1+b)\ln b.\eta(-12b\eta + b\eta^2 -$$
$$12C_1 + 12bC_1 + 12b^2C_1 - 12b^3C_1)\ln\eta -$$
$$18C_1(-1+b^2)\ln^2 b.\eta\ln\eta +$$
$$36(-1+b)^2 b(-\eta+\eta^2)\ln^2\eta +$$
$$18(-1+b)b\ln b.\eta\ln^2\eta]/[18(-1+b)^2(2-2b+(1+b)\ln b)^2]$$

Thus the boundary derivative $f''(1)$ is fined analytically as below:

$$f''(1) = \frac{2\sqrt{b}[\ln b - (b+1)]}{(b-1)[2(b-1)-(b+1)\ln b]} + \tag{17}$$
$$Re f_1''(1) + O(Re^2)$$

A comparison between the analytical and numerical results of $f''(1)$ for Re=0.1 and different values of *b* has been presented in Table 1.

Analytical solution of the steady energy equation when the temperature at the wall is constant leads to the following dimension-less function $\theta(\eta)$:

$$\theta(\eta) = \frac{\int_\eta^b \frac{1}{\chi}\exp(RePr.\int_\chi^b \frac{f(t)}{t}dt)d\chi}{\int_1^b \frac{1}{\chi}\exp(RePr.\int_\chi^b \frac{f(t)}{t}dt)d\chi} \tag{18}$$

By calculating the dimensionless temperature gradient and heat flux at the wall, the Nusselt number is expressed as follows:

$$Nu = \frac{2Rq''_w}{k(T_w - T_\infty)} = -4\theta'(1) \tag{19}$$

Analytical and numerical results of the Nusselt number for Re=0.1 and different values of the Prandtl number are reported in Table 2.

Inverse problem

All inverse solutions for minimizing an objective function are based on an optimization method. One such method is the Levenberg–Marquardt algorithm which is an iterative method for solving nonlinear least-squares problems of parameter estimation.

This algorithm is recommended for solving nonlinear parameter estimation problems. Also, it is used for ill-posed linear problems [58]. Therefore, it is used in this paper for the estimation of the unknown parameters of time-dependent wall heat flux.

The main steps of the Levenberg–Marquardt inverse method are the sensitivity analysis, iteration process, convergence criterion, and calculation algorithms as discussed below.

The inverse problem is the estimation of time-dependent wall heat flux using the transient temperature values measured by a sensor. Thus, $aq_w(\tau)/2k$,(in which *a* is the cylinder radius and *k* is the fluid thermal conductivity with known values), is unknown and time-dependent whereas the transient temperature $Y(\tau)$ is the measured transient temperature in the sensor position within the time interval of $0 \le \tau \le \tau_f$.

Table 1: Comparison of numerical and analytical results of f"(1).

b	f"(1)	
	Analytical results	Numerical Results
1.1	650.352	650.475
2	11.001	11.012
10	0.6674	0.6687

Table 2: Analytical and numerical results of Nusselt number for Re=0.1.

Pr		b		
	1.1		2	
	Analytical result	Numerical result	Analytical result	Numerical result
0.7	42.40	42.57	6.27	6.32
7	46.26	46.48	10.08	10.29
70	78.88	79.23	22.36	22.47
700	181.82	182.16	48.52	48.74

The measured temperatures in the sensor position at times τ_i, i= 1,2,...,$I$are used to estimate$aq_w(\tau)/2k$. To solve this inverse problem, we consider the unknown heat flux function $a\ q_w(\tau)/2k$ to be parameterized in the following general linear form:

$$a\,q_w(\tau)/2k = \sum_{j=1}^{N} P_j C_j(\tau) \qquad (20)$$

Where P_j are the unknown parameters and$C_j(\tau)$are known trial functions, e.g. polynomials, spline, etc. with N parameters. For this inverse heat transfer problem, parameters P should be estimated. For this purpose, the differences between measured and calculated temperatures are formed as an objective function to be minimized.

Several methods exist to develop an objective function, one of which is the least-square method as defined below [59]:

$$S_p = \sum_{i=1}^{I} [Y_i - T_i(P)]^2 \qquad (21)$$

Where$S_p$is the sum of the squares error and hence the objective function. To solve this inverse heat transfer problem and estimate N unknown parameters P_j, j= 1,2,..., N, the objective function S_p should be minimized. Eq. (15), $P^T = [P_1, P_2, \ldots P_I]$ is the vector of unknown parameters. Also, $T_i(P) = T(P,\tau_i)$ and $Y_i = Y(\tau_i)$are the estimated and measured temperatures at the time τ_i, respectively. The estimated temperature T_i (P) is obtained from the solution of the direct problem (9, 12) at the measurement (sensor) point using the unknown parameters P_j, j= 1,2,..., N.

Sensitivity analysis

Before solving the inverse problem, it is useful to analyze it and the estimated parameter's sensitivities to unknown parameters. This analysis can yield a metric for the best position of the temperature sensor and a criterion for the stability of the inverse solution. The sensitivity coefficients representing the estimated temperature sensitivity to small parameter variations are defined as (22).

$$J_{ij} = \frac{T_i(P_1, P_2, \ldots, P_j + \varepsilon P_j, \ldots, P_N) - T_i(P_1, P_2, \ldots, P_j, \ldots, P_N)}{\varepsilon P_j} \qquad (22)$$

Where$\varepsilon = 10^{-6}$.

The coefficients of (22) comprise the elements of the sensitivity matrix J.

$$J(P) = \left[\frac{\partial T^T(P)}{\partial P}\right]^T = \begin{bmatrix} \frac{\partial T_1}{\partial P_1} & \frac{\partial T_1}{\partial P_2} & \cdots & \frac{\partial T_1}{\partial P_N} \\ \frac{\partial T_2}{\partial P_1} & \frac{\partial T_2}{\partial P_2} & \cdots & \frac{\partial T_2}{\partial P_N} \\ \vdots & \vdots & \cdots & \vdots \\ \frac{\partial T_I}{\partial P_1} & \frac{\partial T_I}{\partial P_2} & \cdots & \frac{\partial T_I}{\partial P_N} \end{bmatrix} \qquad (23)$$

Where N and I are the total numbers of unknown parameters and the total number of measurements, respectively.

With small sensitivity coefficients, the inverse problem is so-called an ill-posed problem meaning that the inverse problem is sensitive to measurement errors and an accurate estimation of the parameters cannot be achieved. Thus, coefficients with high absolute values, leading to stable inverse analysis, are more desirable.

The iterative procedure

The sensitivity matrix is a nonlinear function of the vector of unknown parameters. Therefore, an iterative procedure is used to linearize the vector of estimated values. This process is carried out through Tailor series expansion around the current value P^k at iteration k, as [60]:

$$P^{k+1} = P^k + \left[(J^k)^T J^k + \mu^k \Omega^k \right]^{-1} (J^k)^T \left[Y - T(P^k) \right] \quad (24)$$

Where μ^k is a positive scalar value named damping parameter and Ω^k is a diagonal matrix. $\mu^k \Omega^k$ is the damping parameter matrix used to dampen the oscillations and instabilities resulting in the ill-conditioned character of the inverse problem. A large value is assumed for this parameter at the beginning of the iteration process because the problem is generally ill-posed around the initial guess chosen for the iteration process. This parameter can be far from the actual parameters. As a result, at the beginning of the iteration, the Levenberg–Marquardt method tends toward the steepest descent method in which a very small step is taken in the negative gradient direction. Then, as the iteration continues the value of μ^k is reduced making the Levenberg–Marquardt method perform similarly to the Newton-Gauss method.

Convergence criterion

To the convergence of Equation (24), a convergence criterion is needed to stop the iteration procedure of the Levenberg-Marquardt method. This criterion prevents the expansion of the measured errors and together with the iteration algorithm as a regularization technique, changes the inverse problem into a well-conditioned problem. The following convergence criterion is used in this study:

$$S(P^{k+1}) < \varepsilon_1 \quad (25)$$

Where ε_1 is the selected tolerance for stopping the minimization process, as chosen by the user based on the distortion amount of the measured data. This criterion examines whether the objective function using the obtained solution is adequately minimized.

Computational algorithm

Assuming an initial guess of P^0 for the unknown parameter vector P and k=0 and μ_0= 0.05, Levenberg–Marquardt algorithm is summarized in the following steps:

1. Solve the direct problem using the initial guess for P^k, i.e. the initial guess for wall temperature, to obtain the temperature vector $T(P^k) = (T_1, ..., T_I)$.

2. Calculate $S(P^k)$ using Equation (21).

3. Calculate the sensitivity matrix J^k defined by equation (23) and diagonal matrix Ω^k using the current P^k values. To calculate the diagonal matrix Ω^k, use the following relation.

$$\Omega^k = diag[(J^k)^T J^k] \quad (26)$$

4. Solve the following linear system of algebraic equations, obtained from the iteration of (24).

$$\left[(J^k)^T J^k + \mu^k \Omega^k \right] \Delta P^k = (J^k)^T [Y - T(P^k)] \quad (27)$$

5. Calculate the new estimation P^{k+1} as:

$$P^{k+1} = P^k + \Delta P^k \quad (28)$$

6. Solve the direct problem using the new estimate P^{k+1} and get the vector $T(P^{k+1})$ and then calculate $S(P^{k+1})$ using equation (21).

7. If $S(P^{k+1}) \geq S(P^k)$, then substitute μ^k with $10\mu^k$ and return to step 4.

8. If $S(P^{k+1}) \leq S(P^k)$, accept the new estimate P^{k+1} and substitute μ^k with $0.1\mu^k$.

9. Check the stopping criterion (25). Stop the iterative procedure if it is satisfied. Else, substitute k with k+1 and return to step 3.

RESULTS AND DISCUSSION

Estimation of the unknown wall heat flux in stagnation point flow on the cylinder, using the Levenberg-Marquardt method with no information about unknown functions is the main aim of this research.

The implicit Finite Difference method is used to discretize the governing equations. The time variable is assumed dimensionless and the time step is considered $\Delta\tau$ = 0.01.

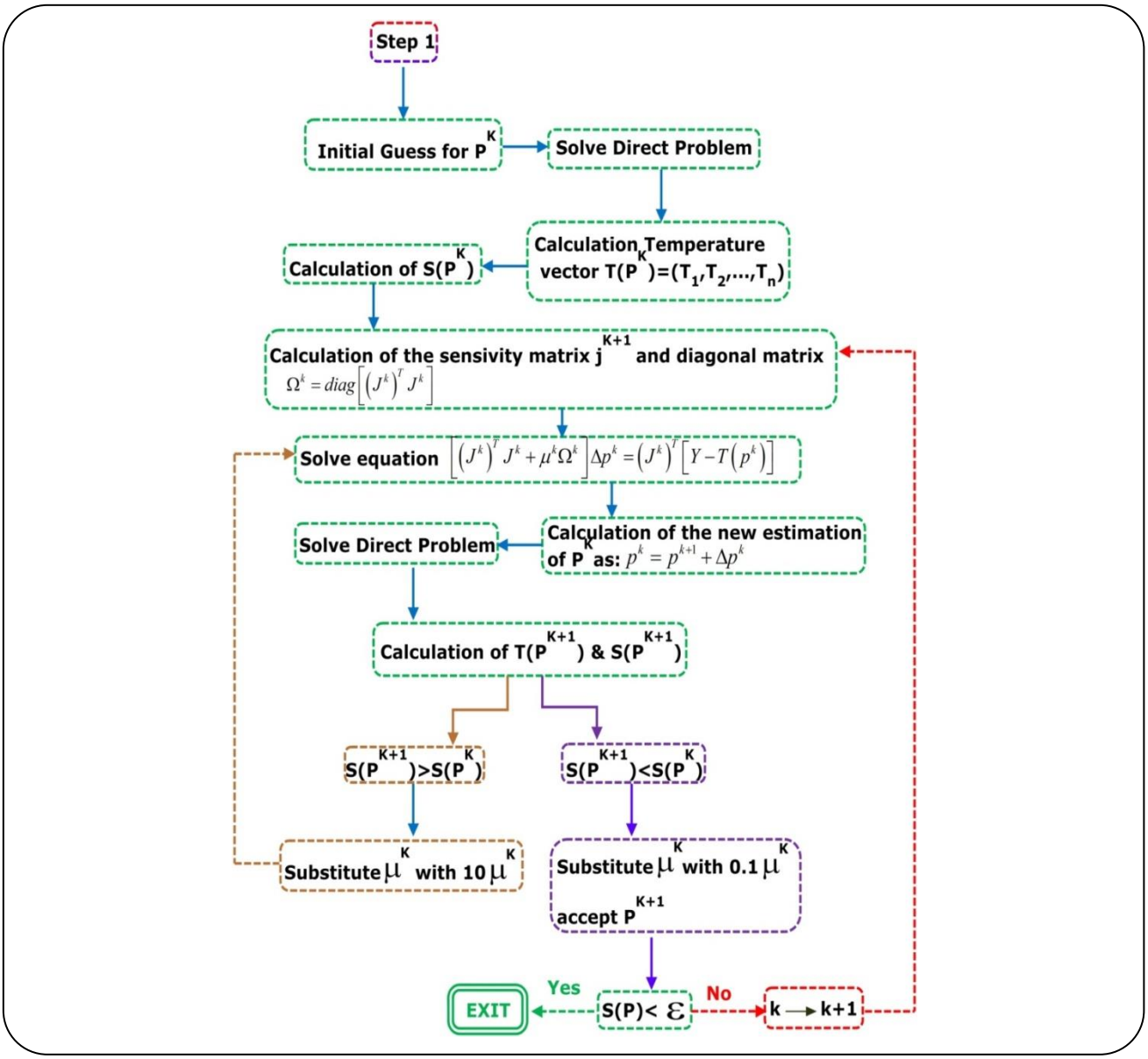

In this study, using the measured temperature at a point, the boundary heat flux is estimated and the noise data sensitivity is evaluated. Noisy data are generated using (29). The stability of the proposed approach against different noise levels is analyzed withσ = 0.01 T_{max} and σ = 0.03 T_{max}.

$$Y(\tau_i) = Y_{ex}(\tau_i) + \omega\,\sigma \tag{29}$$

In the above equation,$\sigma$is the standard deviation of the measurement errors, and $\omega$is a random variable with normal distribution, zero mean and unitary standard deviation. For the present study,-2.576≤ω≤2.576. Also, for noisy data, the relation $\varepsilon_1 = \sigma^2\tau_f$ is considered where the final dimensionless time parameter is $_f$. To evaluate the accuracy of the proposed algorithm, exponential, sinus–cosine, triangular and trapezoidal functions are examined for ($aq_w(\tau)$ / 2k).

Detailed descriptions for the time-dependent wall heat flux are shown as follows:

$$\frac{aq_w(\tau)}{2k} = 300e^{\tau} - 55.5e^{2\tau} \tag{30}$$

$$\frac{aq_w(\tau)}{2k} = 10 + 500\sin(\tau) + 200\cos(3\tau) \tag{31}$$

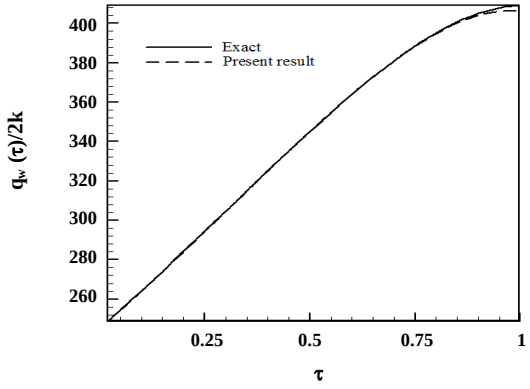

Fig. 3: Calculated heat flux with Re=100 vs. the exact heat flux in the form of an exponential function.

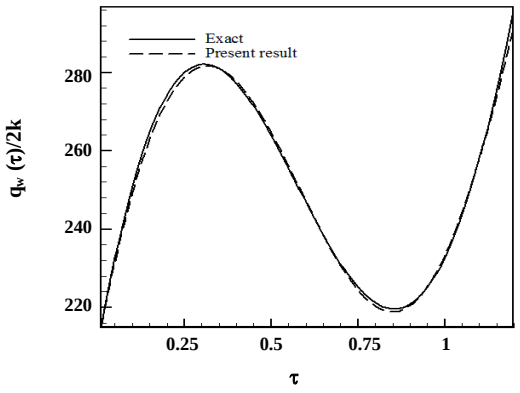

Fig. 5: Calculated heat flux with Re=100 vs. the exact heat flux in the form of a sinus–cosine function.

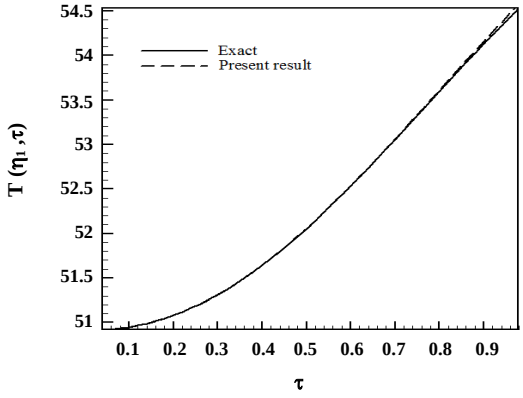

Fig. 4: Temperature history at the point η_1 = 1.05 with Re=100 for calculated heat flux vs. exact heat flux in the form of an exponential function.

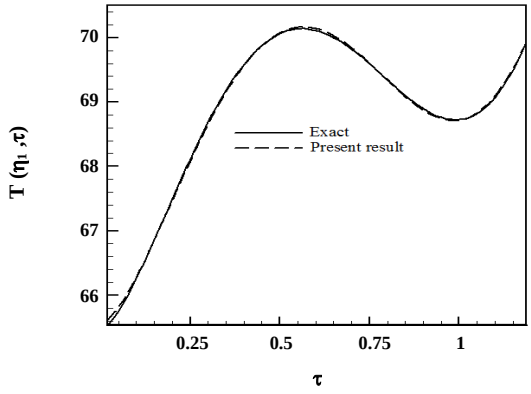

Fig. 6: Temperature history at the point η_1= 1.025 with Re=100 for calculated heat flux vs. exact heat flux in the form of a sinus–cosines function.

$$\frac{a q_w(\tau)}{2k} = \begin{cases} 200+300\tau & for \quad 0 < \tau \le 0.6 \\ 497-200\tau & for \quad \tau > 0.6 \end{cases} \tag{32}$$

$$\frac{a q_w(\tau)}{2k} = \begin{cases} 150 & for \quad 0 < \tau \le 0.2 \\ 50+500\tau & for \quad 0.2 < \tau \le 0.4 \\ 250 & for \quad 0.4 < \tau \le 0.6 \\ 550-500\tau & for \quad 0.6 < \tau \le 0.8 \\ 150 & for \quad \tau > 0.8 \end{cases} \tag{33}$$

Also, temperature history at points η_1 is presented for the above values as well as the estimated values.

Figures 3 through 10 show the above functions as well as those calculated using the inverse method in selected values of Reynolds number and then the inverse solution with the noisy data is presented. As expected, in cases estimated by triangular and trapezoidal functions, sharp corner points on the curves make the estimation more difficult and increase the RMS error.

The Root Mean Square (RMS) error, as a suitable measure for evaluating the accuracy of the Levenberg–Marquardt parameter estimation, is defined as follows:

$$e_{RMS} = \sqrt{\frac{1}{I}\sum_{i=1}^{I}\left[\frac{a q_w(\tau_i)_{est}}{2k} - \frac{a q_w(\tau_i)_{ex}}{2k}\right]^2} \tag{34}$$

Where $a q_w(\tau_i)_{est}/2k$ is the estimated function at the time τ_i, $a q_w(\tau_i)_{ex}/2k$ is the exact function at the time τ, $_i$ and I is the number of measurements. The RMS error is a measure to represent the difference between

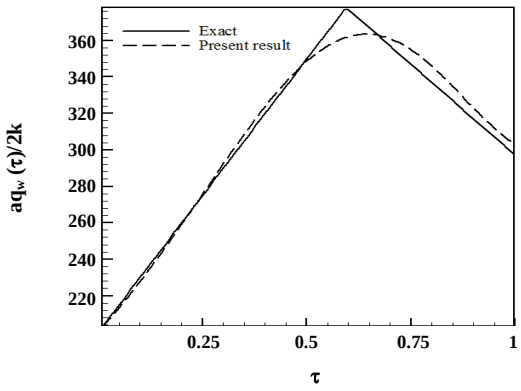

Fig. 7: Calculated heat flux with Re=200 vs. the exact heat flux in the form of a triangular function.

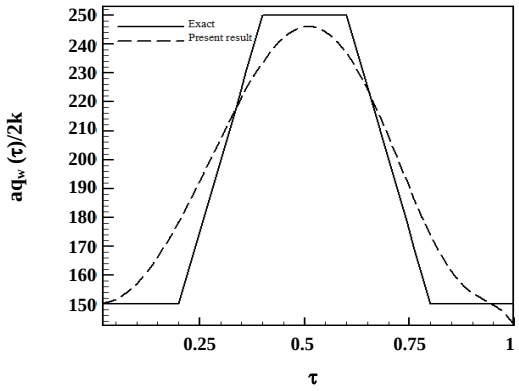

Fig. 9: Calculated heat flux with Re=500 vs. the exact heat flux in the form of a trapezoidalfunction.

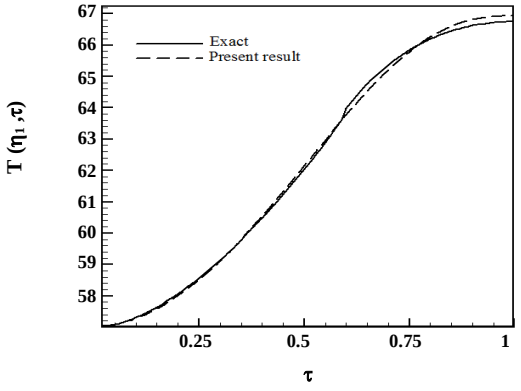

Fig. 8: Temperature history at the point η_1 = 1.025with Re=200 for calculated heat flux vs. exact heat flux in the form of triangular function.

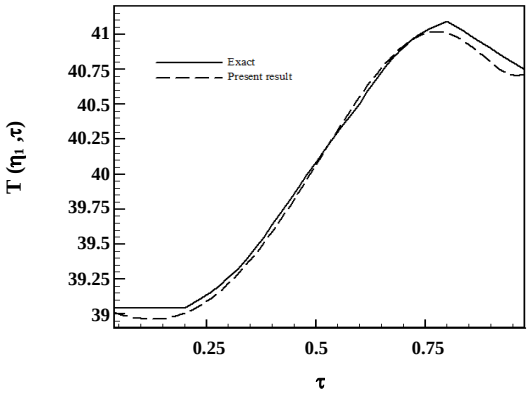

Fig. 10: Temperature history at the point η_1 = 1.03 with Re=500 for calculated heat flux vs. exact heat flux in the form of trapezoidal function.

The estimated and actual function values. It is observed through the obtained results that the RMS error is the highest for trapezoidal function due to sharp corner points in the function curve. As witnessed in the following curves and table as well as the calculated errors, the proposed approach demonstrates acceptable accuracy.

The effect of noisy data on the time-dependent heat flux estimation is shown in Figs. 11–18.

The deviation of the estimated heat flux from the real wall heat flux increased when the standard deviation of measurement errors increased from $\sigma=0.01T_{max}$ to $\sigma=0.03T_{max}$ and as can be seen noisy data leads to more deviation of the obtained results compared to the exact data because according to the Equation (29), noise in measured data by the sensor leads to error in Eq. (21). Also, the RMS errors related to these results are given in Table 3.

As can be seen in the tables, the error values for estimating triangular and trapezoidal functions are higher than exponential and Sinus-cosines functions because high gradient changes are not completely recovered by the estimation function and some oscillations are observed near the singular points. We note that functions containing discontinuities and sharp comers (i.e., discontinuities on their first derivatives) are the most difficult to be recovered by inverse analysis. Generally, the results depend on the physical characteristics of the problem, the number of parameters to be estimated, the initial guess, etc.

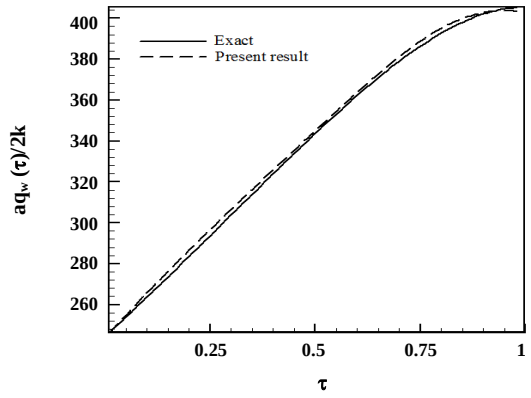

Fig. 11: Calculated heat flux with Re=100 with noisy data (σ = 0.01 T_{max}) vs. the exact heat flux in the form of an exponential function.

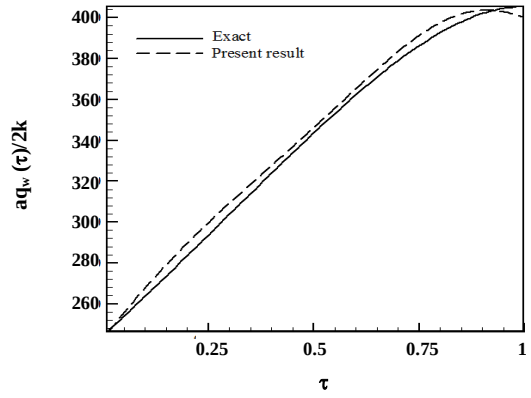

Fig. 12: Calculated Heat flux with Re=100 with noisy data (σ = 0.03 T_{max}) vs. the exact heat flux in the form of an exponential function.

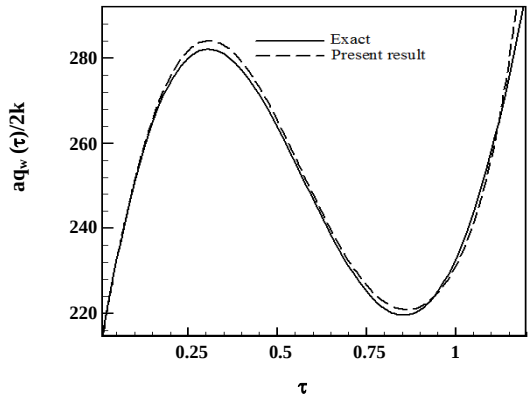

Fig. 13: Calculated heat flux with Re=100 with noisy data (σ = 0.01 T_{max}) vs. the exact heat flux in the form of a sinus–cosine function.

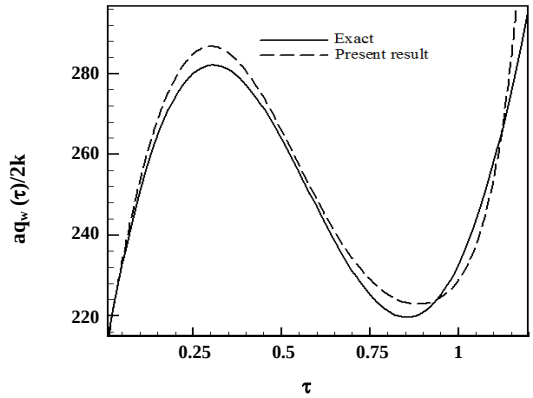

Fig. 14: Calculated Heat flux with Re=100 with noisy data (σ = 0.03 T_{max}) vs. the exact heat flux in the form of a sinus–cosine function.

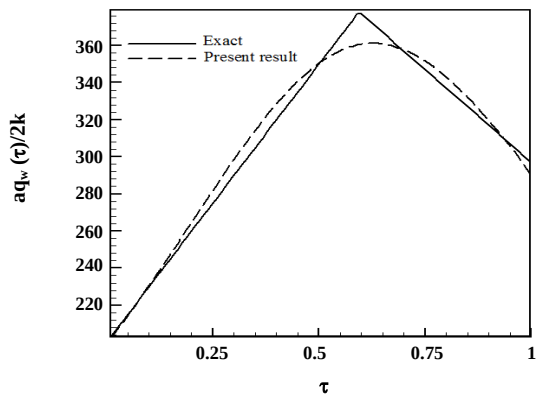

Fig. 15: Calculated heat flux with Re=200 with noisy data (σ= 0.01 T_{max}) vs. the exact heat flux in the form of a triangular function.

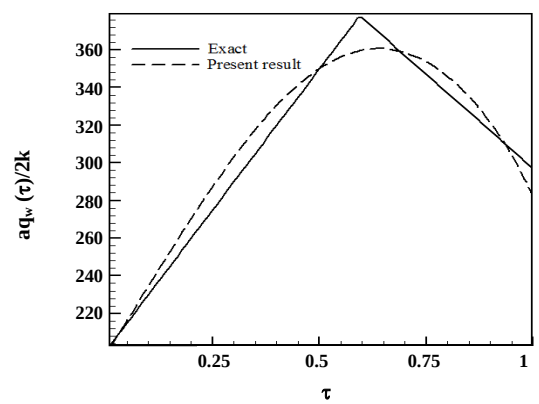

Fig. 16: Calculated Heat flux with Re=200 with noisy data (σ= 0.03 T_{max}) vs. the exact heat flux in the form of a triangular function.

Table3:Calculated RMS error for different approximation functions of heat flux with noisy data.

Function	e_{RMS}		
	σ=0	σ=0.01Tmax	σ=0.03Tmax
Exponential	0.0092	0.107	0.203
Sinus–cosine	0.094	0.121	0.291
Triangular	0.365	0.397	0.481
Trapezoidal	0.388	0.412	0.489

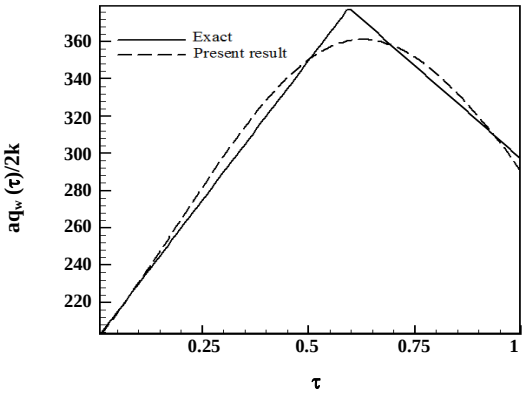

Fig. 17: Calculated heat flux with Re=500 with noisy data (σ = 0.01 T_{max}) vs. the exact heat flux in the form of a trapezoidal function.

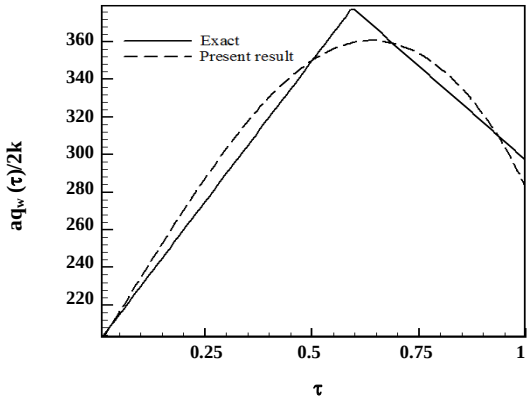

Fig. 18: Calculated Heat flux with Re=500 with noisy data (σ = 0.03 T_{max}) vs. the exact heat flux in the form of a trapezoidal function.

CONCLUSIONS

In this paper, a semi-similar solution to axisymmetric inverse problems based on the measured temperature distribution at a point in the stagnation region is presented for the estimation of time-dependent heat flux. To estimate the unknown boundary condition, the ninth-order polynomials function with coefficients obtained by Levenberg–Marquardt parameter estimation algorithm has been used. The RMS error was calculated for different examples. The major results of this paper can be summarized as follows:

- By comparing the sensitivity coefficients at Re = 100, it results that the maximum and minimum values of the sensitivity coefficients are 0.1619 and 5.62×10^{-6}, respectively which is related to exponential and triangular heat flux therefore, the exponential heat flux shows the lowest sensitivity to the P_j parameters, and the triangular heat flux has the highest sensitivity to these parameters.
- The maximum RMS error values for σ = 0, σ = $0.01T_{max}$ and σ = $0.03T_{max}$ are 0.388, 0.412 and 0.489, respectively, which were obtained to estimate the trapezoidal heat flux. These results show that if there are non-derivative points in the unknown function, the accuracy of the parameter estimation method decreases.
- The RMS error increases with increasing the number of non-derivative points in the heat flux functions.
- Based on the studied cases and by comparing the obtained heat flux with the exact values and the fact that no prior data is required regarding the structure of the unknown function, and considering the acceptable stability against noisy data, it is concluded that this approach is an effective method for estimating the time-dependent heat flux.

Nomenclature

a	Cylinder radius, m
C	Known trial functions used in Levenberg-Marquardt method
e_{RMS}	Root mean square error
f	Dimensionless function defining velocity field
I	Number of measurements
J	Sensitivity matrix
k	Thermal conductivity, W/(m.K)

$\bar{k}$	Free stream strain rate, 1/s
N	Number of unknown parameters
P	Fluid pressure, N/m^2
p	Dimensionless pressure
P^k	Vector of unknown parameters at current iteration
r, z	Cylindrical coordinates, m
Re	Reynolds number
T	Temperature, °C
u	Radial component of the velocity field, m/s
w	Axial component of the velocity field, m/s
t	Time,s
T_∞	Free stream temperature, °C
$q_w(t)$	Time-Dependent wall heat flux, W/m^2
Y	Measured transient temperature in the sensor position,°C
η	Dimensionless radius
θ	Dimensionless temperature
τ	Dimensionless time
μ	Dynamic viscosity,$(N.s)/m^2$
μ^k	Damping parameter
υ	Kinematic viscosity, m^2/s
ρ	Fluid density,kg/m^3
$\bar{\alpha}$	Fluid thermal diffusivity coefficient, m^2/s
σ	Standard deviation of measurement errors
ω	Normal distribution
Ω^k	Diagonal matrix
ε_1	Tolerance for stopping the minimization process

Received : Aug. 1, 2020 ; Accepted : Dec. 14, 2020

REFERENCES

[1] Huang C. H., Wang P., A Three-Dimensional Inverse HeatConduction Problem in Estimating Surface Heat Flux by ConjugateGradient Method, *Int. J. Heat Mass Trans.*,**42(18)**: 3387-3403 (1999).

[2] Shiguemori E.H., Harter F.P., Campos Velho H.F., Dasilva J.D.S., Estimation of Boundary Condition in Conduction Heat Transfer by Neural Networks, *Tendências em Matemática Aplicada e Computacional*.**3**: 189-195(2002).

[3] Volle F., Maillet D., Gradeck M., Kouachi A., Lebouché M., Practical Application of Inverse Heat Conduction for Wall Condition Estimation on a Rotating Cylinder, *Int. J. Heat Mass Trans.*, **52(2)**: 210-221 (2009).

[4] Golbahar HaghighiM.R., EghtesadM., MalekzadehP., NecsulescuD.S., Three-Dimensional Inverse Transient Heat Transfer Analysis of Thick Functionally Graded Plates, *Ene. Convers. Manage*, **50(3)**: 450-457 (2009).

[5] Su J., Neto A., Two Dimensional Inverse Heat Conduction Problem of Source StrengthEstimation in Cylindrical Rods, *Applied Mathematical Modeling.*, **25(10)**: 861- 872 (2001).

[6] Hsu P.T., Estimating the Boundary Condition in a 3D Inverse Hyperbolic Heat Conduction Problem, *Applied Mathematics and Computation*, **177(2)**: 453- 464 (2006).

[7] Shi J., Wang J., Inverse Problem of Estimating Space and Time Dependent Hot Surface Heat Flux in Transient Transpiration Cooling Process, *Int. J. Thermal Sc*., **48(7)**: 1398-1404 (2009).

[8] Ling X., Atluri S.N., Stability Analysis for Inverse Heat Conduction Problems, *Computer Modeling in Engineering & Sciences.*, **13(3)**:219-228 (2006).

[9] Jiang B.H., Nguyen T.H., Prud'homme M., Control of the Boundary Heat Flux During the Heating Process of a Solid Material, *Int. Commun. Heat Mass Transfer.*, **32(6)**: 728-738 (2005).

[10] Chen S.G., Weng C.I., Lin J., Inverse Estimation of Transient Temperature Distribution in the End Quenching Test, *J. Mater. Process. Technol.*, **86(3)**: 257-263 (1999).

[11] Plotkowski A., Krane M.M., The Use of Inverse Heat Conduction Models for Estimation of Transient Surface Heat Flux in Electroslag Remelting, *J. Heat Transfer*., **137(3)**:031301 (2015).

[12] Hsu P.T., Wang S. G., Li T.Y., An Inverse Problem Approach for Estimating the Wall Heat Flux in Film Wise Condensation on a Vertical Surface with Variable HeatFlux and Body Force Convection, *Applied Mathematical Modeling.*, **24(3)**: 235-245 (2000).

[13] Khaniki H.B., Karimian S.M.H., Determining the Heat Flux Absorbed by Satellite Surfaces with Temperature Data,*Journal of Mechanical Science and Technology*., **28**: 2393-2398 (2014).

[14] Beck J., Black well B., Clair C. St., "Inverse Heat Conduction", John Wiley & Sons, Inc., New York, (1985).

[15] Liu F. B., A Hybrid Method for The Inverse Heat Transfer of Estimating Fluid ThermalConductivity and Heat Capacity, *Int. J. Thermal Sc*., **50(5)**: 718-724 (2011).

[16] Mohammadiun M., Rahimi A.B., Khazaee I., Estimation of the Time-Dependent Heat Flux Using Temperature Distribution at a Point by Conjugate Gradient Method, *Int. J. Thermal Sc.*, **50(11)**: 2443-2450 (2011).

[17] Tai B.L., Stephenson D.A., Shih A.J., An Inverse Heat Transfer Method for Determining Work Piece Temperature in Minimum Quantity Lubrication Deep Hole Drilling, *J. Manuf. Sci. Eng.*, **134(2)**: 021006 (2012).

[18] Rahimi A.B., Mohammadiun M., Estimation of the Strength of the Time-Dependent Heat Source Using Temperature Distribution at a Point in a Three Layer System, *Int. J. Eng.*, **25(4)**:389-397 (2012).

[19] Mohammadiun H., Molavi H., Talesh Bahrami H.R., Mohammadiun M., Real-Time Evaluation of Severe Heat Load Over Moving Interface of Decomposing Composites, *J. Heat Transfer.*, **134(11)**: 111202 (2012).

[20] Mohammadiun M., Molavi H., Talesh Bahrami H.R., Mohammadiun H., Application of Sequential Function Specification Method in Heat Flux Monitoring of Receding Solid Surfaces, *Heat Transfer Eng.*, **35(10)**: 933–941(2014).

[21]WuT. S., LeeH. L.,Chang W.J.,Yang Y.C., An Inverse Hyperbolic Heat Conduction Problem in Estimating Pulse Heat Flux with a Dual-Phase-Lag Model, *Int. Commun. Heat Mass Transfer.*,**60**: 1-8 (2015).

[22] Cuadrado D. G., Marconnet A., Paniagua G., Non-Linear Non-Iterative Transient Inverse Conjugate Heat Transfer Method Applied to Microelectronics, *Int. J. Heat Mass Trans.*,**152**: 119503 (2020).

[23] Duda P., Simplification of 3D Transient Heat Conduction by Reducing it to an Axisymmetric Heat Conduction Problem and a New Inverse Method of the Problem Solution, *Int. J. Heat Mass Trans.*,**143**: 118492 (2019).

[24] Huang S., Tao B., Li J., Yin Z., On-Line Heat Flux Estimation of a Nonlinear Heat Conduction System with Complex Geometry Using a Sequential Inverse Method and Artificial Neural Network, *Int. J. Heat Mass Trans.*,**143**: 118491 (2019).

[25] Brociek R., Słota D., Król M., Matula G., Kwaśny W., Comparison of Mathematical Models with Fractional Derivative for the Heat Conduction Inverse Problem based on the Measurements of Temperature in Porous Aluminum, *Int. J. Heat Mass Trans.*, **143**: 118440 (2019).

[26] Perakis N., Strauß J., Haidn O.J., Heat Flux Evaluation in a Multi-Element CH_4/O_2Rocket Combustor Using an Inverse Heat Transfer Method, *Int. J. Heat Mass Trans.*, **142**: 118425 (2019).

[27] Sochinskii A., Colombet D., Medrano Muñoz M., Ayela F., Luchier N., Flow and Heat Transfer around a Diamond-Shaped Cylinder at Moderate Reynolds Number, *Int. J. Heat Mass Trans.*, **142**: 118435 (2019).

[28]Hiemenz K., Die Grenzchicht an Einem in den Gleichformingen Flussigkeitsstrom Eingetauchten Geraden Kreiszylinder, *Dingler's Polytechn. Journal*, **326**: 391-393 (1911).

[29]Homann F. Z., Der Einfluss Grosser Zahighkeit bei der Strmung um Den Zylinder und um Die Kugel, *Zeitschrift für Angewandte Mathematik und Mechanik*, **16**: 153-164 (1936).

[30] Howarth L., The Boundary Layer in Three Dimensional Flow. Part II. The Flow Near a Stagnation Point, *Philos. Mag.*, **42(7)**: 1433-1440 (1951).

[31] Davey A., Boundary Layer Flow at a Saddle Point of Attachment, *J. Fluid Mech.*, **10(4)**: 593-610 (1961).

[32] Wang C., Axisymmetric Stagnation Flow on a Cylinder, *Q. Appl. Math.*, **32(2)**: 207-213 (1974).

[33] Gorla R.S.R., Nonsimilar Axisymmetric Stagnation Flow on a Moving Cylinder, *Int. J. Eng. Sci.*, **16(6)**: 397-400 (1978).

[34] Gorla R.S.R., Transient Response Behaviour of an Axisymmetric Stagnation Flow on a Circular Cylinder due to Time Dependent Free Stream Velocity, *Int. J. Eng. Sci.*, **16(7)**: 493- 502 (1978).

[35] Gorla R.S.R., Heat Transfer in Axisymmetric Stagnation Flow on a Cylinder, *Appl. Sci. Res.*, **32(5)**: 541-553 (1976).

[36] Gorla R.S.R., Unsteady Viscous Flow in the vicinity of an Axisymmetric Stagnation-Point on a Cylinder, *Int. J. Eng. Sci.*, **17(1)**: 87-93 (1979).

[37] Cunning G.M., Davis A.M.J., Weidman P.D., Radial Stagnation Flow on a Rotating Cylinder with Uniform Transpiration, *J. Eng. Math.*, **33(2)**: 113-128 (1998).

[38] Takhar H.S., Chamkha A.J., Nath G., Unsteady Axisymmetric Stagnation-Point Flow of a Viscous Fluid on a Cylinder, *Int. J. Eng. Sci.*, **37(15)**: 1943-1957 (1999).

[39] Saleh R., Rahimi A.B., Axisymmetric Stagnation-Point Flow and Heat Transfer of a Viscous Fluid on a Moving Cylinder with Time-Dependent Axial Velocity and Uniform Transpiration, *J. Fluids Eng.*, **126(6)**: 997–1005 (2004).

[40] Rahimi A.B., Saleh R., Axisymmetric Stagnation-Point Flow and Heat Transfer of a Viscous Fluid on a Rotating Cylinder with Time-Dependent Angular Velocity and Uniform Transpiration, *J. Fluids Eng.*, **129(1)**: 107–115 (2007).

[41] Rahimi A.B., Saleh R., Similarity Solution of Unaxisymmetric Heat Transfer in Stagnation-Point Flow on a Cylinder with Simultaneous Axial and Rotational Movements, *J. Heat Transfer*, **130(5)**: 054502-1–054502-5 (2008).

[42] Abbasi A.S., Rahimi A.B., Non-Axisymmetric Three-Dimensional Stagnation-Point Flow and Heat Transfer on a Flat Plate, *J. Fluids Eng*., **131(7)**: 074501.1– 074501.5 (2009).

[43] Abbasi A.S., Rahimi A.B., Three-Dimensional Stagnation- Point Flow and Heat Transfer on a Flat Plate with Transpiration, *J. Thermophys. Heat Transfer*, **23(3)**: 513–521 (2009).

[44] Abbasi A.S., Rahimi A.B., Niazmand H., Exact Solution of Three-Dimensional Unsteady Stagnation Flow on a Heated Plate, *J. Thermophys. Heat Transfer*, **25(1)**: 55–58 (2011).

[45] Abbasi A.S., Rahimi A.B., Investigation of Two-Dimensional Stagnation-Point Flow and Heat Transfer Impinging on a Flat Plate, *J. Heat Transfer*, **134(6)**: 064501-1-o64501-5 (2012).

[46] Mohammadiun H., Rahimi A.B., Stagnation-Point Flow and Heat Transfer of a Viscous, Compressible Fluid on a Cylinder, *J. Thermophys. Heat Transfer*, **26(3)**: 494-502 (2012).

[47] Mohammadiun H., Rahimi A.B., Kianifar A., Axisymmetric Stagnation-Point Flow and Heat Transfer of a Viscous Compressible Fluid on a Cylinder with Constant Heat Flux, *Sci. Iran., Trans. B*, **20(1)**: 185–194 (2013).

[48] Rahimi A.B., Mohammadiun H., Mohammadiun M., Axisymmetric Stagnation Flow and Heat Transfer of a Compressible Fluid Impinging on a Cylinder Moving Axially, *J. Heat Transfer*, **138(2)**: 022201-1-022201-9 (2016).

[49] Rahimi A.B., Mohammadiun H., Mohammadiun M., Self-Similar Solution of Radial Stagnation Point Flow and Heat Transfer of a Viscous, Compressible Fluid Impinging on a Rotating Cylinder, *Iran. J. Sci. Technol. Trans. Mech. Eng.*, **43(1)**: S141-S153 (2019).

[50]Mohammadiun H., Amerian V., Mohammadiun M., Rahimi A.B., Similarity Solution of Axisymmetric Stagnation-Point Flow and Heat Transfer of a Nanofluid on a Stationary Cylinder with Constant Wall Temperature, *Iran. J. Sci. Technol. Trans. Mech. Eng.*,**41(1)**: 91-91 (2017).

[51] Mohammadiun H., Amerian V., Mohammadiun M., Khazaee I., Darabi M., Zahedi M., AxisymmetricStagnation-Point Flow and Heat Transfer of Nano-Fluid Impingingon a Cylinder with Constant Wall Heat flux, *Thermal Science*, **23(5)**:3153-3164 (2019).

[52] Zahmatkesh R., Mohammadiun H., Mohammadiun M., Dibaei Bonab M.H., Investigation of Entropy Generation in Nanofluid's Axisymmetric Stagnation Flow over a Cylinder with Constant Wall Temperature and Uniform Surface Suction-Blowing, *Alexandria Eng. J.*, **54(4)**: 1483-1498 (2019).

[53] Alizadeh R., Gomari S. R., Alizadeh A., Karimi N., Li L..K.B., Combined Heat and Mass Transfer and Thermodynamic Irreversibilities in the Stagnation-Point Flow of Casson Rheological Fluid over a Cylinder with Catalytic Reactions and Inside a Porous Medium under Local Thermal Nonequilibrium, *Computers and Mathematics with Applications*. (2020).[In Press]

[54] Bilal M., Sharma S., Aneja M., Cattaneo-Christov Heat Flux Model of Eyring Powell Fluid Along with Convective Boundary Conditions, *Iran. J. Chem. Chem. Eng. (IJCCE)*, **40 (3)**:971-979 (2021).

[55] Nematollahzadeh A., Jangara H., Exact Analytical and Numerical Solutions for Convective Heat Transfer in a Semi-Spherical Extended Surface with Regular Singular Points, *Iran. J. Chem. Chem. Eng. (IJCCE)*, **40 (3)**:980-989 (2021).

[56] Madelatparvar M., Hosseini salami M., Abbasi F., Numerical Study on Parameters Affecting the Structure of Scaffolds Prepared by Freeze-Drying Method, *Iran. J. Chem. Chem. Eng. (IJCCE)*,**39(2)**: 271-286 (2020).

[57] Hussain Z., Zaman M., Nadeem M., Ullah A., CFD Modeling of the Feed Distribution System of a Gas-Solid Reactor, *Iran. J. Chem. Chem. Eng. (IJCCE)*, **38(1)**: 233-242 (2019).

[58] Ozicik M.N., Orlande H.R.B., "Inverse Heat Transfer Fundamentals and Application", Taylor & Francis, New York, (2000).

[59] Azimi A., "Thermo-Hydraulically Simulation of Thermal Systems Using Inverse Evaluation", Ph.D Thesis, Sharif University of Technology, Tehran, Iran. (In Persian) (2007).

[60] Beck J.V., Arnold K.J., "Parameter Estimation in Engineering and Science", John Wiley & Sons, Inc., New York, (1977).

[61] Hong L., Wang C.Y., Annular Axisymmetric Stagnation Flow on a Moving Cylinder, *Int. J. Eng. Sci.*, **47(1)**: 141–152 (2009).

[62] Zahmatkesh R., Mohammadiun H., Mohammadiun M., Dibaei Bonab M.H., Sadi M., Theoretical Investigation of Entropy Generation in Nanofluid's Axisymmetric Stagnation Flow over a Cylinder with Constant Wall Heat Flux and Uniform Surface Suction-Blowing, *Iran. J. Chem. Chem. Eng. (IJCCE)*, **40(6)**: 1893-1908 (2021).

[63] Cuadrado D. G., Marconnet A., Paniagua G., Non-linear Non-Iterative Transient Inverse Conjugate Heat Transfer Method Applied to Microelectronics, *Int. J. Heat Mass Trans.*, **152**: 119503 (2020).

[64] Ashraf M., Ali K., Numerical Simulation of Micropolar Flow in a Channel under Osciatory Pressure Gradient**,** *Iran. J. Chem. Chem. Eng. (IJCCE)*, **39(2)**: 261-270 (2020).

[65] Safaei H., Sohrabi M., Falamaki C., Royaee S.J., A New Mathematical Model for the Prediction of Internal Recirculation in Impinging Streams Reactors, *Iran. J. Chem. Chem. Eng. (IJCCE)*,**39 (2)**: 249-259 (2020).

[66] Habibi M. R., Amini M., Arefmanesh A., Ghasemikafrudi E., Effects of Viscosity Variations on Buoyancy-Driven Flow from a Horizontal Circular Cylinder Immersed in Al_2O_3-Water Nanofluid, *Iran. J. Chem. Chem. Eng. (IJCCE)*, **38(1)**: 213-232 (2019).